INL/CON-23-72486-Revision-0

Sensitivity of ATF Experiments in the Center Flux Trap of the Advanced Test Reactor to Adjacent Experiments

August 2023

Changing the World's Energy Future

Travis J Labossiere-Hickman, Tristen Jeda Rogers, Michael Jason Worrall, Mehmet Turkmen

Idaho National Laboratory

INL/CON-23-72486-Revision-0

Sensitivity of ATF Experiments in the Center Flux Trap of the Advanced Test Reactor to Adjacent Experiments

Travis J Labossiere-Hickman, Tristen Jeda Rogers, Michael Jason Worrall, Mehmet Turkmen

August 2023

Idaho National Laboratory
Idaho Falls, Idaho 83415

http://www.inl.gov

Prepared for the
U.S. Department of Energy
Under DOE Idaho Operations Office
Contract DE-AC07-05ID14517, DE-AC07-05ID14517

Sensitivity of ATF Experiments in the Center Flux Trap of the Advanced Test Reactor to Adjacent Experiments

T. J. Labossiere-Hickman, T. J. Rogers, M. J. Worrall, and M. Turkmen
Idaho National Laboratory
2525 N. Fremont Ave., Idaho Falls, Idaho 83415

Travis.LabossiereHickman@INL.gov, Tristen.Rogers@INL.gov,
Michael.Worrall@INL.gov, Mehmet.Turkmen@INL.gov

ABSTRACT

Irradiation experiments conducted in the Idaho National Laboratory's Advanced Test Reactor are typically assumed to have little effect on one another. This assumption does not hold true for certain experiments in close proximity. To evaluate the impacts on safety and programmatic parameters of experiments in the center flux trap, the contents of the adjacent H and inner-A positions were modeled with a range of possible irradiation targets. First, neutron flux maps with experiments in those positions were compared against a baseline configuration. Next, several safety and programmatic parameters for a generic accident-tolerant fuel test train were calculated. It was shown that these parameters can exhibit considerable sensitivity to the contents of the H and A experiment positions.

KEYWORDS: accident-tolerant fuels, advanced test reactor, irradiation experiments, sensitivity

1. INTRODUCTION

In response to the 2011 incident at Japan's Fukushima Daiichi nuclear power plant, the United States Department of Energy initiated the Accident-tolerant Fuel (ATF) program to develop safer light water reactor (LWR) fuels and claddings [1]. ATF technologies require extensive laboratory testing prior to commercial deployment. ATF-2, an ongoing series of irradiation experiments being performed at Idaho National Laboratory (INL), was designed to test ATF prototypes and provide conditioning and burnup extension of previously irradiated commercial fuel pins [2].

The ATF-2 series is being irradiated in Loop 2A of the Center Flux Trap (CFT) in INL's Advanced Test Reactor (ATR). The design of ATR is such that the experiment positions are relatively independent of one another, enabling the power or contents of one part of the reactor to be altered without producing any significant observable impact on the power or contents of other parts of the reactor. However, a number of positions are in close proximity to each other, and they often contain strong absorbers. Two such cases are the H and inner-A positions, which are located between the ATR driver fuel and the CFT (Fig. 1).

Typically, the experiment design and corresponding safety analysis are conducted long before the final loading of the reactor has been established. Irradiation testing is subject to last-minute replacement and alternation of experiments. In the present paper, we evaluate how potential adjacent irradiation targets can impact the safety and programmatic parameters of ATF experiments.

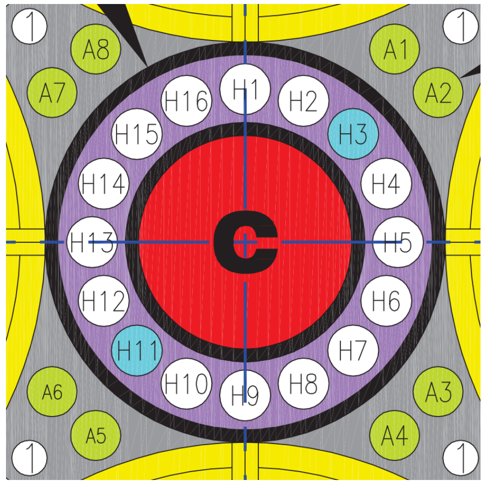

Figure 1: Center Flux Trap, Surrounded by the H and Inner-A Positions

2. METHODS

2.1. Analysis Software

The Monte Carlo N-Particle Transport Code System Version 6.2 (MCNP6.2) [3] was used to perform the neutron transport simulations for this study. Those simulation results provided neutron fluxes, reactivity worths, fission heating rates, and other reaction rates.

The depletion projection was performed using the ORIGEN from the SCALE 6.2.4 package [4]. SCALE/ORIGEN was coupled to MCNP via the MCNP-ORIGEN Activation Automation tool (MOAA) developed at INL [5].

MCNPTools [6] was used to post-process the mesh tally files. The open-source data visualization tool ParaView was then applied to create the flux and relative difference plots.

2.2. Assumptions

It is assumed that ATR can be modeled as a fixed-source problem. A characteristic neutron source originating in the reactor driver fuel was imposed. The energy distribution was the Watt fission spectrum. The source spatial distribution and shim positions were obtained from a reactor engineering calculation for early Cycle 169A (i.e., the most recent cycle at time of submission).

2.3. Reaction Rate Normalization

MCNP tally results are reported per unit source particle. To convert tally results to absolute neutron fluxes and reaction rates, it is necessary to normalize to the average neutrons per fission ν, average energy per fission ε, and core power observed by the lobe (i.e., the lobe-adjusted total core power [LATCP]). This LATCP value serves to normalize the reaction rates in a given lobe to the overall power distribution. See Eq. 1 for the Center (C) LATCP calculation, given the assumed power Q_C, tally result $(\texttt{f7:n})_C$, and tally mass m_C:

$$LATCP(C) = \frac{Q_C}{(\texttt{f7:n})_C \times m_C} \sum_{i=1}^{5} (\texttt{f7:n})_i m_i \tag{1}$$

Neutron flux calculations were performed using `f4` tallies, normalized as shown in Eq. 2:

$$\phi = \frac{\nu}{\varepsilon}(LATCP)(\texttt{f4:n}) \tag{2}$$

Fission heating rates were calculated using `f7` tallies (MeV/g) multiplied by masses (Eq. 3). The `f7` tally conservatively assumes local energy deposition, as per the requirements of the ATR Safety Analysis Report (SAR) [7].

$$Q = \frac{\nu}{\varepsilon}(LATCP)(\texttt{f7:n}) \times m \tag{3}$$

For given reaction x and number density N, one-group cross sections (1GXS) were calculated using `f4` tallies with the `fm4` multiplier. The normalization cancels out of the numerator and denominator, giving Eq. 4:

$$\Sigma_x = \left(\frac{\texttt{fm4}(x) \times \texttt{f4:n}}{\texttt{f4:n}}\right) N \tag{4}$$

2.4. Flux Mapping

Neutron flux perturbations due to experiments in the H and inner-A positions were evaluated using fine-grid mesh tallies superimposed over the CFT and surrounding regions. The neutron flux was tallied over three energy groups: 0 eV < thermal ≤ 0.625 eV < epithermal ≤ 1 MeV < fast, with sufficient histories to produce statistics acceptable for plotting.

2.5. Sample Experiment

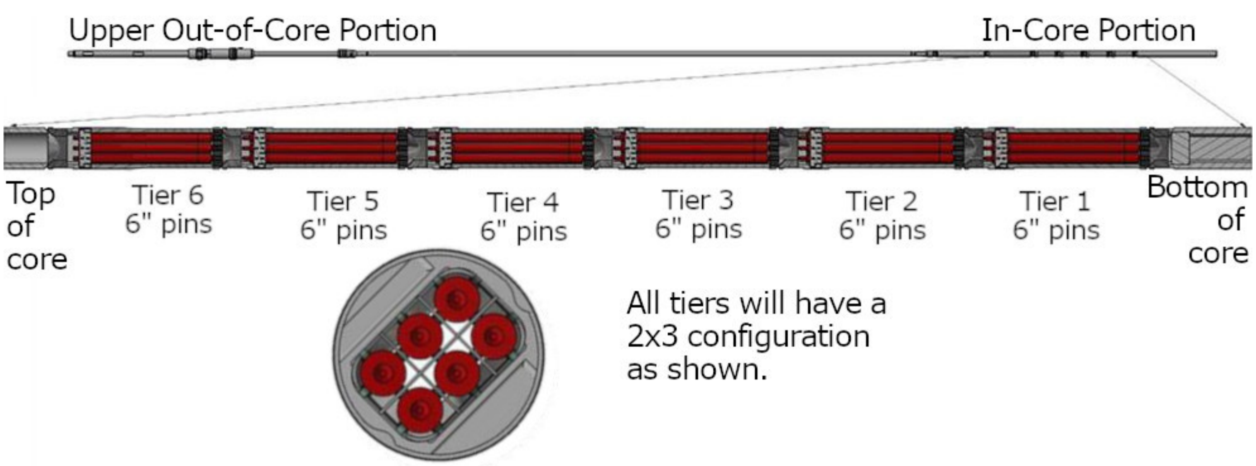

Figure 2: In-core Portion of the ATF-2Pert Test Train.

An example test train (TT) was designed. The model (hereafter referred to as “ATF-2Pert”) was based on real ATF-2 experiments [2], [8]. It was simplified by replacing all proprietary samples with generic, identical light-water reactor fuel samples and excluding heterogeneities such as shrouds and instrumentation. The ATF-2Pert TT comprises six tiers of six rodlets apiece, as shown in Fig. 2. Each rodlet is approximately 6 in. tall and contains a 4-in. stack of 10 fuel pellets. Fluxes and heating rates were tallied over all 360 pellets. Further information on the design and applications of the tiered ATF-2Pert generic TT can be found in [9].

One safety consideration for irradiation testing in the ATR is the reactivity worth ρ of an experiment. Each cycle's core saftey analysis package assumptions remain valid so long as the combined worths of experiments versus their respective backups remain within $\pm 0.25\$$. For a given target configuration, the ρ_0 of ATF-2Pert versus a backup assembly is calculated, as are their reactivities versus a baseline configuration (ρ_{ATF} and ρ_{BU}, respectively).

The SAR for the ATR [7] places a limit of 200 kW fission power on fueled experiments in the CFT. For ATF experiments, this is typically the limiting safety criterion. Typical programmatic requirements include rodlet linear heat generation rate (LHGR), burnup, and neutron fast fluence.

2.6. Sample Targets

A grid of H and A position irradiation targets was defined. A subset of the experiments analyzed is tabulated in Section 3. Solid flow restrictor outboard position (SFROP) fillers, high specific activity (HSA) cobalt, low specific activity (LSA) cobalt, neptunium (Np) oxide, and hafnium (Hf) are actual targets previously irradiated in those positions [10]. Others (e.g., B_4C control rods, helium, and water) are purely academic in nature.

2.7. Cross Section Scoping

The response of an experiment to perturbations in an irradiation position depends on the neutron cross sections (XS) of that position. It is hypothesized that 1GXS may be used as a proxy to estimate the sensitivity of experiment parameters to a particular adjacent target swap.

To that end, homogenized materials for five irradiation targets were defined. These materials comprised all nuclides within the H and inner-A positions over the height of the ATR driver fuel. Each target was placed in all the H and inner-A positions. The flux, total reaction rate (MT=1), and absorption reaction rate (MT=-2) were tallied in the MCNP model using the `f4` and `f4m` cards and the respective smeared material. The 252-group and one-group macroscopic total XS Σ_t and absorption XS Σ_a were then calculated according to Eq. 4.

3. RESULTS

3.1. Base Configuration

A base model representing one of the most common target layouts was selected. This base configuration features instrumentation and fillers in the H-3 and H-11 positions, HSA cobalt in the other H positions, and LSA cobalt in the A positions (see Fig. 3 and the first row of Table 1).

3.2. Flux Profile Perturbations

Flux distributions were tallied for all cases. Several comparisons are shown and discussed here. Note that the color scales on the relative difference plots have been adjusted to emphasize the effects in the CFT; the flux difference in the H or A positions themselves lies significantly outside the bounds in all cases.

Fig. 4 compares an all-LSA cobalt case to the base case. Replacing the H positions' HSA cobalt with LSA causes a major flux depression in their vicinity, with the thermal flux in the CFT decreasing from around 7% at the core midplane (pictured) to as much as 15% at the ends.

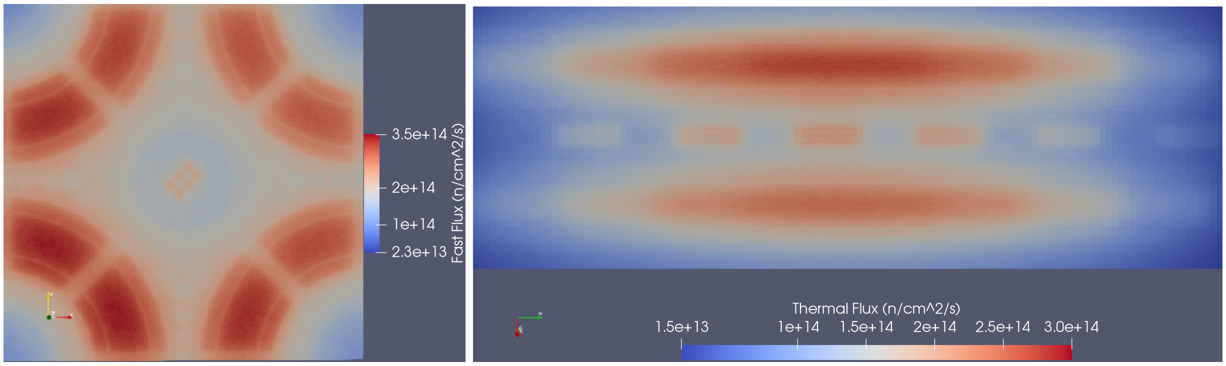

(a) Fast Flux (Radial, Core Midplane) **(b) Thermal Flux (Axial, Centerline)**

Figure 3: Flux Distribution of the Base Configuration

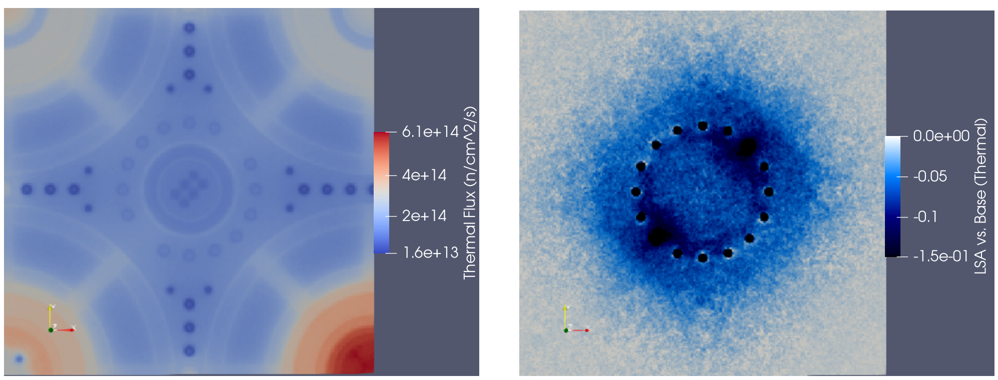

(a) Thermal Flux (Base) **(b) Relative Difference (LSA vs. Base)**

Figure 4: Thermal Flux Perturbation from LSA Cobalt (Core Midplane)

Fig. 5 illustrates a perturbation to just the inner-A positions. On the left-hand side is the total flux distribution with LSA cobalt in all the H and inner-A positions. Swapping the contents of the eight inner-A positions for HSA cobalt produces a several-percent flux increase in their vicinity, extending into the CFT. These two configurations are represented by the second and third rows of Table 1, respectively.

Following a cycle of depletion, there is a flux shift from the core midplane toward the top and bottom (Fig. 6), but little change on average. This flux profile flattening is expected due to burnup of the ATR driver fuel. Because the driver fuel is highly enriched, however, the flux spectrum changes very little on average, having negligible effects on ATF-2 sensitivities. The perturbation due to neckshim (control rod) insertion, located in a cruciform arrangement beyond the inner-A positions, can be seen to be fairly localized.

3.3. Experiment Parameters

Due to space limitations, the full set of ATF-2 experiment safety and programmatic parameters and perturbation cases could not be included. A subset of these parameters and cases is provided in Table 1. Tier 3, the closest to the core midplane, is the peak tier in terms of LHGR.

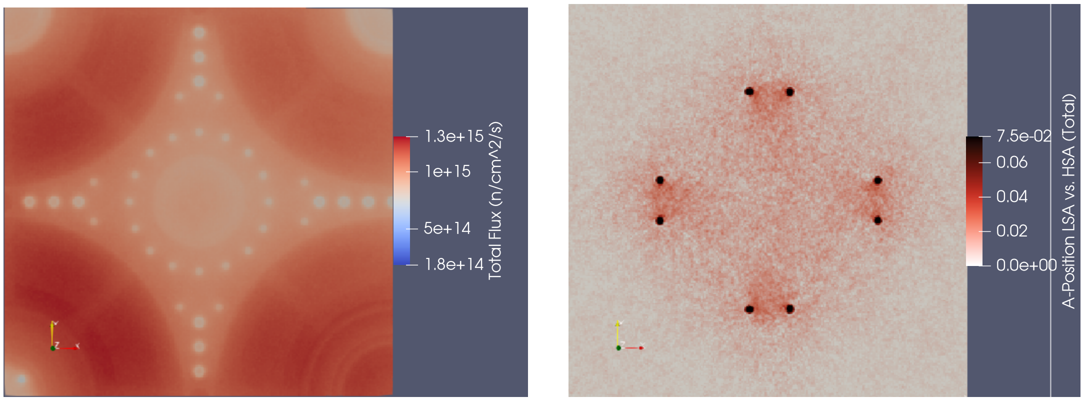

(a) Total Flux (LSA in A) **(b) Relative Difference (HSA vs. LSA in A)**

Figure 5: Total Flux Perturbation from HSA Cobalt in Inner-A (Upper Core)

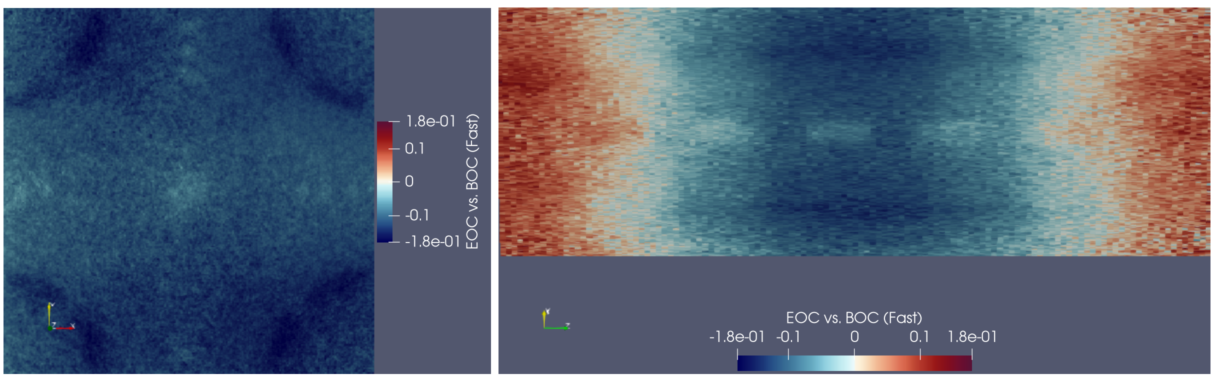

(a) Fast Flux Difference (Radial, Midplane) **(b) Fast Flux Difference (Axial, Centerline)**

Figure 6: Perturbation from Cycle Depletion

Note that ATF-2Pert is higher-power than historical ATF-2 experiments. The actual experiments incorporated hafnium neutron shields to tailor tiers' LHGR to the desired ranges, as well as instrumentation and additional structural material. The optimal thickness of this hafnium shielding is dependent on the assumed contents of the adjacent positions.

3.4. One-Group Cross-Sections

The 252-group and one-group XS of the homogenized materials were generated and plotted in Fig. 8. Their values are presented in Table 2. The XS do not satisfactorily capture the effects of their respective targets upon ATF-2Pert. As shown for TT power and thermal flux in Fig. 7, the relationship of the parameters of interest to the 1GXS is neither linear nor monotonic.

Note that only the H-position results have been shown. The inner-A position results have marginally lower XS due to a faster neutron spectrum, but are essentially the same.

Table 1: Selected Numerical Results of Several H and Inner-A Experiment Perturbations.

Inner-A contents	H contents	TT Power (kW)	Tier 3 LHGR (W/cm)	Thermal Flux (frac)	Fast Flux (frac)	ρ_{ATF} (\$)	ρ_{BU} (\$)	ρ_0 (\$)
LSA	HSA	181.9	643.9	0.1114	0.2204	0	0	$+0.36627$
LSA	LSA	171.8	612.1	0.1081	0.2190	-0.78764	-0.74822	$+0.32685$
HSA	LSA	173.5	617.3	0.1086	0.2193	-0.47625	-0.44657	$+0.33659$
HSA, LSA	HSA, LSA	176.8	626.7	0.1095	0.2199	-0.25508	-0.23967	$+0.35087$
HSA	HSA, LSA	177.4	628.8	0.1097	0.2196	-0.13990	-0.12391	$+0.35029$
HSA	HSA	181.5	640.5	0.1108	0.2207	$+0.21691$	$+0.21389$	$+0.36929$
Np	HSA	181.9	642.8	0.1119	0.2214	$+0.10370$	$+0.09731$	$+0.37267$
Np	Np	187.3	664.3	0.1170	0.2237	-0.12465	-0.13367	$+0.37529$
HSA	Np	186.5	660.9	0.1158	0.2230	-0.04429	-0.05149	$+0.37347$
HSA	B_4C	181.9	648.6	0.1175	0.2245	-0.82824	-0.80590	$+0.34392$
Np	B_4C	182.0	650.1	0.1185	0.2252	-0.91512	-0.89602	$+0.34717$
B_4C	Np	186.4	661.5	0.1176	0.2243	-0.49715	-0.49839	$+0.3675$
B_4C	HSA	181.2	641.0	0.1125	0.2220	-0.26619	-0.25643	$+0.35651$
B_4C	SFROP	198.5	711.9	0.1212	0.2220	$+0.79658$	$+0.73199$	$+0.43086$
HSA	B_4C, Hf	146.3	519.7	0.0936	0.2191	-2.02876	-1.91365	$+0.25117$
HSA	HSA, Np	183.6	648.9	0.1129	0.2217	$+0.09956$	$+0.09731$	$+0.36852$
HSA	LSA, Np	179.3	636.5	0.1117	0.2210	-0.28981	-0.27598	$+0.35244$
B_4C	B_4C	180.9	645.9	0.1189	0.2257	-1.26933	-1.24350	$+0.34044$
H_2O, Np	H_2O, Np	213.7	763.6	0.1367	0.2281	$+0.62675$	$+0.51970$	$+0.47333$
H_2O	H_2O	237.3	853.3	0.1539	0.2318	$+1.39719$	$+1.20388$	$+0.55958$
SFROP	SFROP	202.2	725.5	0.1213	0.2207	$+1.88765$	$+1.79599$	$+0.45793$

4. CONCLUSIONS

Although it is generally assumed that experiments in other ATR positions can be neglected, it is vital to the ATF-2 program to quantify the nearest positions. As evidenced by Figs. 3–5, changeout of irradiation targets in positions near the CFT of the ATR can result in significant perturbations on experiments inside the flux trap, because they perturb the flux incident on the trap from the reactor driver fuel. This can cause considerable variation in the safety and programmatic parameters for ATF experiments. Table 1 can be used to estimate the effect of a potential adjacent target swap. For instance, one sees that moving from an (LSA, HSA) arrangement to an (HSA, Np) arrangement will be relatively benign.

As one would expect, the H positions have a greater impact on the experiment than do the inner-A positions due to their proximity. (See Table 3 for their distances in terms of approximate neutron mean free paths.) This can be seen from the flux perturbations in Figs. 4–5. For a case with the same number of replaced targets, consider the first and fifth rows of Table 1. Both configurations have eight LSA cobalt targets located in different positions, with the latter configuration exhibiting a lower heating rate and reactivity worth.

Table 2: One-Group Cross-Sections for Smeared Experiments.

Test Specimen Type	$\Sigma_t(\mathrm{cm}^{-1})$	$\Sigma_a(\mathrm{cm}^{-1})$
SFROP Filler	2.603E-01	1.92232E-03
HSA Cobalt	4.647E-01	3.08824E-02
LSA Cobalt	8.953E-01	7.24997E-02
Neptunium	8.175E-01	2.40104E-01
Moderator	1.051E+00	2.93940E-03

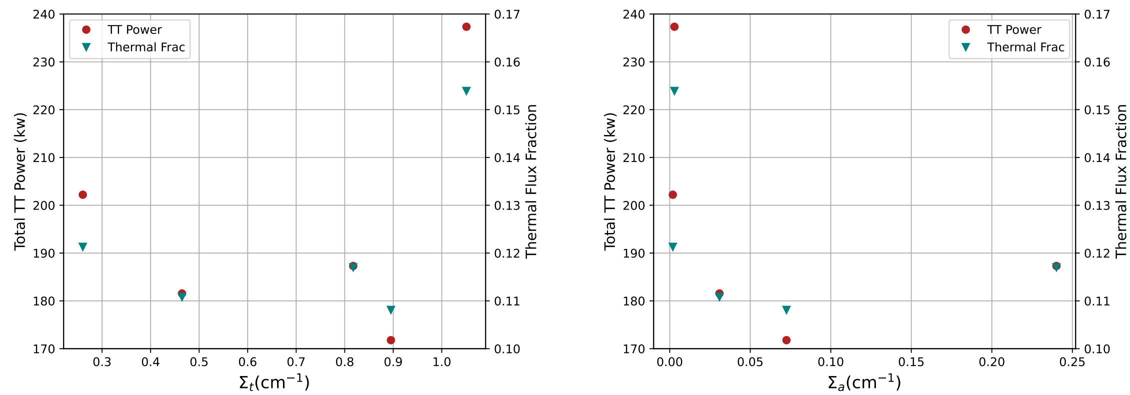

(a) Total **(b) Absorption**

Figure 7: Two Parameters vs. Cross-Section

It is not evident that the impact of an adjacent target can be predicted based solely on its cross-sections. For example, the neptunium target has a higher one-group absorption XS in the H and A positions than does cobalt, but results in a higher thermal flux fraction and total TT fission heating than either cobalt target. The water-filled position is clearly seen to be an outlier, as is expected based on its neutron moderation properties. One can conclude that, to appropriately capture physical effects, it is necessary to explicitly model targets in nearby positions and produce such tables as Table 1.

5. FUTURE WORK

Work is ongoing at INL to quantify the sensitivities of ATF-2C, the latest experiment in the series. The sensitivities are expected to closely resemble those of ATF-2Pert, with key differences in the long, shrouded upper tier.

Future sensitivity and flux mapping studies should be conducted for targets progressively further from the CFT. Perturbing the inner-A positions creates a small but measurable impact. The next positions radially are the neckshim (control rod) penetrations and the driver fuel. The neckshim insertion, driver fuel burnup, and outer shim control cylinder rotation all change during reactor

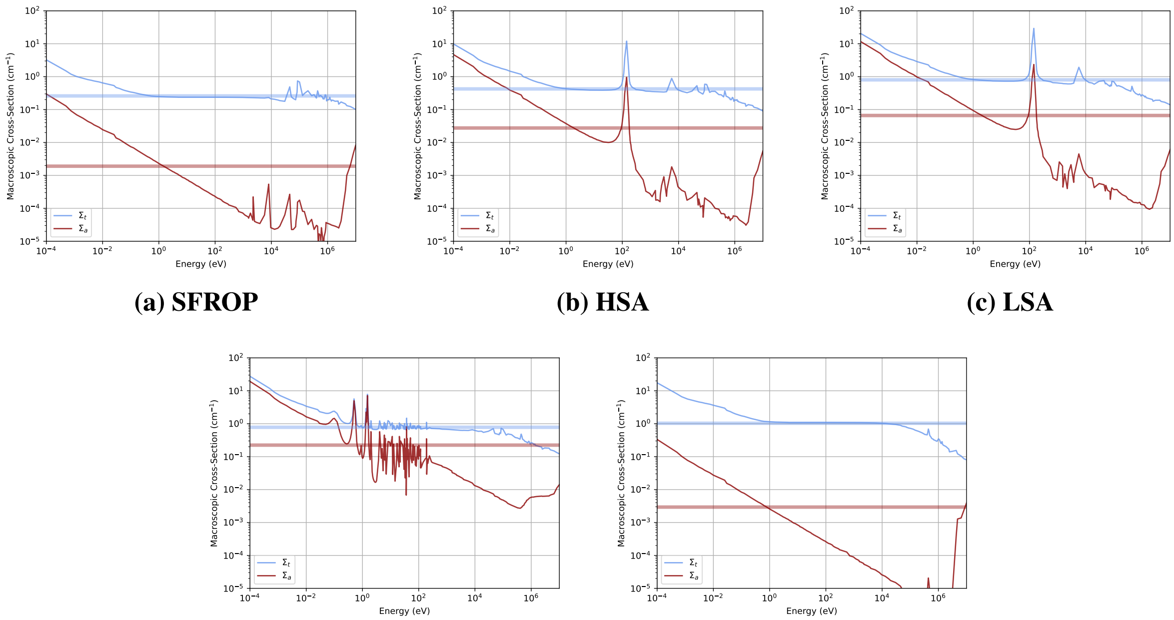

(a) SFROP **(b) HSA** **(c) LSA**

(d) Np **(e) Moderator**

Figure 8: Macroscopic Cross-Sections for Five Targets

Table 3: Number n of mean free paths λ from regions of interest.

Position	**$n\lambda$ from ATF**	**$n\lambda$ from CFT**
H	4.4	2.1
Inner-A	7.2	5.0

operation. Evaluating the sensitivities to each in isolation and combination would be a fruitful area of study. Evaluation of the sensitivities to the other flux traps may be insightful as well.

To the authors' knowledge, the present study is the first sensitivity study of its kind concerning irradiation testing in ATR. Future sensitivity and flux mapping studies should be conducted for fueled experiments in other positions of interest. Such analyses will help ensure the best results for the many diverse irradiation experiments coexisting inside INL's Advanced Test Reactor.

ACKNOWLEDGMENTS

This work was supported through the U.S. Department of Energy Advanced Fuels Campaign under DOE Idaho Operations Office Contract DE-AC07-05ID14517. Accordingly, the U.S. Government retains and the publisher, by accepting the article for publication, acknowledges that the U.S. Government retains a nonexclusive, paid-up, irrevocable, world-wide license to publish or reproduce the published form of this manuscript, or allow others to do so, for U.S. Government purposes.

This research made use of the resources of the High Performance Computing Center at Idaho National Laboratory, which is supported by the Office of Nuclear Energy of the U.S. Department of Energy and the Nuclear Science User Facilities under Contract No. DE-AC07-05ID14517.

REFERENCES

[1] J. Carmack, F. Goldner, S. M. Bragg-Sitton, and L. L. Snead. "Overview of the US DOE accident tolerant fuel development program." Technical report, Idaho National Laboratory, Idaho Falls, ID (United States) (2013).

[2] F. J. Goldner, W. McCaughey, D. M. Wachs, D. Kamerman, C. Jensen, S. L. Hayes, A. Nelson, J. Harp, N. Capps, K. Linton, et al. "The US Accident Tolerant Fuels Program—Update on a National Initiative." (2021).

[3] C. J. Werner et al. "MCNP6.2 Release Notes." Technical Report LA-UR-18-20808, Los Alamos National Laboratory (2018).

[4] W. A. Wieselquist, R. A. Lefebvre, M. A. Jessee, et al. "SCALE Code System." Technical Report ORNL/TM-2005/39, Version 6.2.4, Oak Ridge National Laboratory (2020).

[5] R. Fairhust-Agosta, A. Carter, and J. Peterson-Droogh. "Development of the MCNP-ORIGEN activation automation tool." In *Proceedings of the International Conference on Physics of Reactors-PHYSOR 2022* (2022).

[6] C. R. Bates, S. R. Bolding, C. J. Josey, J. A. Kulesza, C. J. Solomon, Jr., and A. J. Zukaitis. "The MCNPTools Package: Installation and Use." Technical Report LA-UR-22-28935, Los Alamos National Laboratory, Los Alamos, NM, USA (2022). URL https://www.osti.gov/biblio/1884737.

[7] SAR-153. "Chapter 10 – Experiments and Irradiation Facilities – Upgraded Final Safety Analysis Report for the Advanced Test Reactor," Revision 31." Technical Report SAR-153, Idaho National Laboratory (2021).

[8] T. J. Labossiere-Hickman, A. Bascom, B. Durtschi, and D. Kamerman. "ATF-2C Physics Safety and Scoping Analysis." In *Trans. Am. Nucl. Soc*, volume 127. Phoenix, Arizona (2022).

[9] T. J. Rogers, T. Labossiere-Hickman, A. Carter, and M. Turkmen. "The Accident Tolerant Fuels' Neutronics Scoping Study (ATF-2Pert)." In *Trans. Am. Nucl. Soc*, volume 129. Washington, D.C. (2023).

[10] "Nuclear Material Experiments Irradiated in the Advanced Test Reactor." (2022). URL https://nst.inl.gov/irradiationtesting/SitePages/Experiment%20Positions%20in%20Advanced%20Test%20Reactor.aspx.